In situ and in silico evaluation of amine- and folate-terminated dendrimers as nanocarriers of anesthetics

ARTICLE *in* EUROPEAN JOURNAL OF MEDICINAL CHEMISTRY · DECEMBER 2013

Impact Factor: 3.45 · DOI: 10.1016/j.ejmech.2013.11.040 · Source: PubMed

10 AUTHORS, INCLUDING:

Verónica Carrasco Sánchez
University of Talca, Talca, Chile
7 PUBLICATIONS **52** CITATIONS
SEE PROFILE

Jeffrey Comer
Kansas State University
45 PUBLICATIONS **655** CITATIONS
SEE PROFILE

Claudia Sandoval
Universidad Autónoma De Chile
23 PUBLICATIONS **111** CITATIONS
SEE PROFILE

Leonardo Silva Santos
Universidad de Talca
126 PUBLICATIONS **2,226** CITATIONS
SEE PROFILE

European Journal of Medicinal Chemistry 73 (2014) 250–257

Contents lists available at ScienceDirect

European Journal of Medicinal Chemistry

journal homepage: http://www.elsevier.com/locate/ejmech

Original article

In situ and *in silico* evaluation of amine- and folate-terminated dendrimers as nanocarriers of anesthetics

Verónica Carrasco-Sánchez [a], Ariela Vergara-Jaque [a], Matías Zuñiga [a], Jeffrey Comer [b], Amalraj John [a], Fabiane M. Nachtigall [a], Oscar Valdes [a], Esteban F. Duran-Lara [a], Claudia Sandoval [b,**], Leonardo S. Santos [a,*]

[a] Laboratory of Asymmetric Synthesis, Chemistry Institute of Natural Resources, Nanobiotechnology Division at University of Talca, Fraunhofer Chile Research Foundation – Center for Systems Biotechnology, FCR-CSB, Talca University, Talca, P.O. Box 747, Chile
[b] Center for Bioinformatics and Integrative Biology, Universidad Andres Bello, República 239, Santiago, Chile

ARTICLE INFO

Article history:
Received 19 April 2013
Received in revised form
19 November 2013
Accepted 23 November 2013
Available online 12 December 2013

Keywords:
PAMAM dendrimers
Drug delivery
Molecular dynamics
MM-GBSA
MALDI-MS

ABSTRACT

The search for new nano-systems for targeted biomedical applications and controlled drug release has attracted significant attention in polymer chemistry, pharmaceutics, and biomaterial science. Controlled drug delivery has many advantages over conventional drug administration, such as reduction of side effects, maintaining a stable plasma level concentration and improving the quality of life of patients. In this study, PAMAM G5 dendrimers and PAMAM G5-folic acid conjugates (PAMAM G5-FA) are synthesized and characterized by mass spectrometry (MALDI-MS). Controlled release studies at different pH values show that PAMAM G5-FA is a good candidate as a carrier for tramadol and morphine, while mathematical modeling is conducted, suggesting that the release process is governed by a diffusion mechanism. In addition, using molecular dynamics simulations, we investigate the structural and energetic properties that facilitate the encapsulation of tramadol and morphine by unmodified and functionalized PAMAM-G5 dendrimers at low, neutral and high pH. Our results correlate well with experimental data, confirming that tramadol and morphine may be encapsulated both by functionalized PAMAM dendrimers and unmodified PAMAM. Moreover, the simulations further reveal that hydrogen-bond and electrostatic interactions govern the affinity the dendrimers for both drugs. This information is envisioned to prove useful for the encapsulation of other drugs and for the design of novel functionalized dendrimers.

1. Introduction

Dendrimers are hyperbranched three-dimensional macromolecules with globular or ellipsoidal shapes. Relevant properties include their nanoscale size, the presence of hydrophobic or hydrophilic cavities, a wide variety of possible functionalities at their peripheries, and extremely low polydispersity [1,2]. The structure of the dendrimers exhibits significantly novel and distinct physical, chemical, and biological properties in comparison to traditional linear polymers [2–4]. Dendrimers have attracted considerable attention because of wide and almost limitless variations on their chemical structure. There exist numerous methodologies for their synthesis, and their unique structures show characteristic properties, which render them a reliable alternative to traditional polymers in a wide range of applications. One alternative is, the design of new nanocontainers and nanodevices for biomedical applications [1,5], such as drug delivery systems [6,7], antiviral agents, and magnetic resonance imaging contrast agents [8,9]. Among the most frequently used dendrimers in biomedical applications are the poly(amidoamine) (PAMAM) dendrimers, which were first synthesized by Tomalia in 1985, being the most thoroughly investigated and characterized as well as the easiest to obtain commercially [1].

PAMAM dendrimers with different surface functionalities have the ability to encapsulate a wide variety of guest molecules for the purpose of drug delivery. It has been reported that PAMAM dendrimers could be efficient delivery systems with the benefits of enhanced drug solubility, prevention of drug

* Corresponding author. Laboratory of Asymmetric Synthesis, Chemistry Institute of Natural Resources, Nanobiotechnology Division at University of Talca, Fraunhofer Chile Research Foundation – Center for Systems Biotechnology, FCR-CSB, Talca University, Talca, P.O. Box 747, Chile. Tel.: +56 71 201575; fax: +56 71 200448.
** Corresponding author. Center for Bioinformatics and Integrative Biology, Universidad Andres Bello, República 239, Santiago, Chile.
E-mail addresses: claudia.sandoval@unab.cl (C. Sandoval), lssantos@utalca.cl (L. S. Santos).

0223-5234/$ – see front matter © 2013 Elsevier Masson SAS. All rights reserved.
http://dx.doi.org/10.1016/j.ejmech.2013.11.040

degradation, increased circulation time, sustained/controlled drug release and potential drug targeting [10]. In addition, the advances in dendrimer surface engineering, i.e. the conjugation of functional groups to the chain ends of dendrimer surface, could provide stimuli-responsive properties to PAMAM dendritic delivery systems, which could add value to drug delivery efficiency and therapeutic efficacy [11].

The functional groups of amine-terminated PAMAM bind a ligand through hydrogen bonds, electrostatic interactions, and hydrophobic interactions [12–14]. In this study, we examined the interactions between amine- and folate-terminated PAMAM dendrimers of fifth generation and pain relief drug such as morphine and tramadol (Fig. 1). PAMAM dendrimers modified with folic acid (FA) via covalent conjugation neutralize the remaining amines of the dendrimers surfaces, decreases the toxicity of the dendrimers and encapsulate varius drug for targeted therapy [15]. For morphine and tramadol, the conventional pharmaceutical formulations must be administered every four and eight hours, respectively, a frequency which often compromises patient compliance. A modified release formulation would increase the dosage interval and thus reduce fluctuations in circulating concentrations of the drug.

In the present study, folate-terminated PAMAM dendrimers of generation five (PAMAM G5-FA) were prepared by simple chemical modification of PAMAM G5 and evaluated for controlled drug delivery of the common pain relief drugs morphine and tramadol. The driving force that controls the drug release behavior was analyzed by molecular simulation techniques in terms of the structure and energetics of each one of the complexes.

2. Results and discussion

2.1. Polyamine-conjugation of the dendrimers PAMAM G5 with folic acid

The γ-carboxylic acid group of folic acid was covalently conjugated to the free surface amine groups of PAMAM G5 through a carbodiimide mediated amide linkage. A higher molar ratio of 1:140 was used to get all the 128-amine groups of the PAMAM G5 dendrimer conjugated. The conjugates were characterized using mass spectrometry and the spectra shows that only 23 folate molecules were attached to the PAMAM G5 dendrimer (Fig. 2) [16]. The amount of folate was also determined by ^{1}H NMR experiments that showed around 20 units attached to the PAMAM G5 (See Fig. SI4–6 of Supporting information). The amount of molecules coupled to PAMAM G5 likely is due to steric hindrance caused by the size of folic acid.

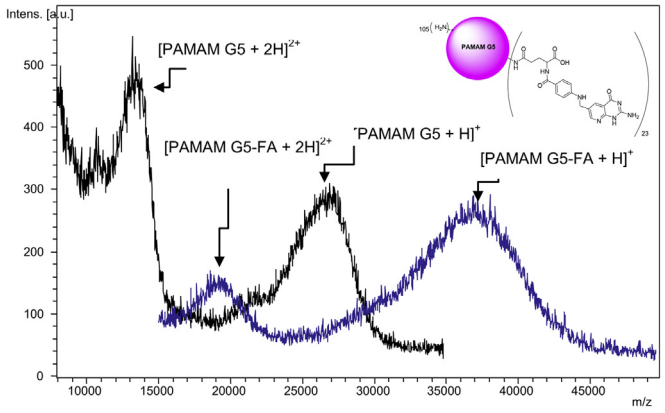

Fig. 2. MALDI-TOF spectra of PAMAM G5 (black) and PAMAM G5-FA (blue) nanocompounds. (For interpretation of the references to color in this figure legend, the reader is referred to the web version of this article.)

2.2. Drug loading into dendrimer conjugates

To determine the capacity of capture of morphine and tramadol on PAMAM G5 and PAMAM G5-FA, an excess of the pharmacological molecule was reacted with a quantity known of dendrimer. Then, by diffusion analysis across a dialysis membrane and UV spectrophotometry analyses at previously determined wavelengths (285 nm for morphine and 270 nm for tramadol), we obtained an indirect estimate of the moles of drug molecules encapsulated by

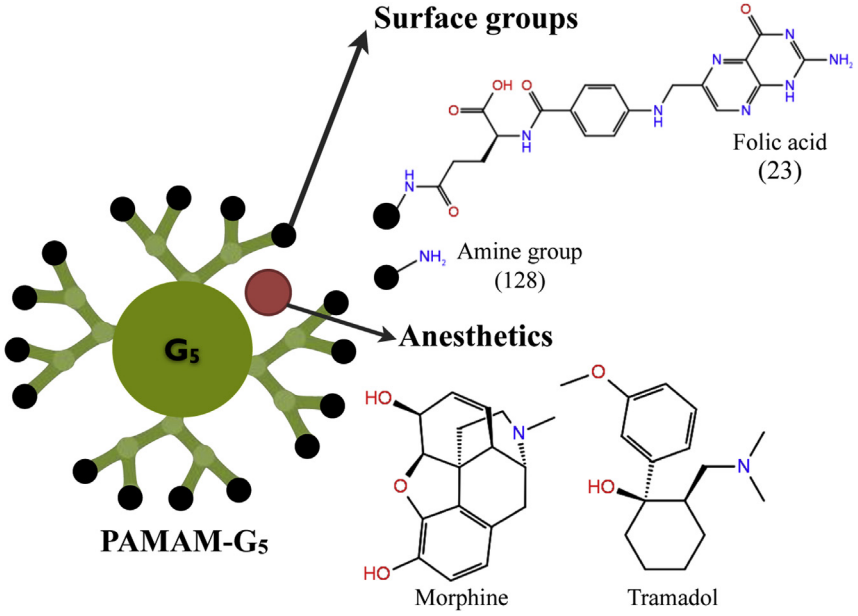

Fig. 1. Schematic representation of amine- and folate-terminated PAMAM dendrimer of generation five and its complexation with the anesthetics: morphine and tramadol. The chemical structures of the surface groups and the drugs are shown at right.

Table 1
Drug loading into amine-terminate PAMAM dendrimer (PAMAM G5) and folate-terminated PAMAM (PAMAM G5-FA).

Dendrimer	Morphine/mol dendrimer	Tramadol/mol dendrimer
PAMAM G5	114	86
PAMAM G5-FA	131	112

every mole of dendrimer. The results obtained are showed in Table 1 (See also Fig. SI7 of Supporting information).

With the results obtained it is possible to conclude, in the first instance, that the two dendrimers studied, PAMAM G5 and PAMAM G5-FA, have the ability to encapsulate morphine and tramadol. However, the folate-terminated dendrimers demonstrate increased drug content and encapsulation efficiency. We attribute this difference to the hydrophobic aromatic groups of the folate molecules. This result is in agreement with the results published by Chandrasekar et al. [17], which suggested that the greater the number of heavy folate moieties attached to the surface amine groups of PAMAM G5, the more space that might be made available to accommodate large numbers of drug molecules. With respect to the non-covalent interaction that proceeds between the pharmacological molecules and dendrimers, different studies were realized [18,19]. These assays have suggested different types of interactions between them, the most common being hydrophobic, electrostatic and ionic interactions between the drug and the dendrimers, all of which depend on the pH.

Our results indicate that both the unmodified and functionalized PAMAM dendrimers have a high capacity to capture molecules, forming non-covalent complexes. The ability to encapsulate molecules into PAMAM dendrimers has been demonstrated in several previous studies, which corroborate our results. Milhen et al. [20] demonstrated that PAMAM G4 encapsulates 40 molecules of ibuprofen and, other study showed that PAMAM G3 and G4 encapsulate 32 and 78 molecules of ibuprofen, respectively [7]. Moreover, the encapsulation of drugs by PAMAM G5-FA has also been described in a study showing the capability of this functionalized PAMAM dendrimer to encapsulate an antitumoral drug 2-metoxiestradiol [15].

Amine- and folate-terminated PAMAM dendrimers are capable of encapsulating a larger number of molecules of morphine than tramadol, due to the fact that tramadol can be found as a racemic mixture of enantiomers, (1*R*,2*R*)-(+)-tramadol and (1*S*,2*S*)-(−)-tramadol [21,22] causing a steric blockage in the surface for entering to the internal cavity of the dendrimers. To understand what happens with regard to the interactions between the dendrimers and the drugs were performed molecular dynamics simulations, which are described below.

2.3. In vitro release profile

The *in vitro* release behavior of morphine and tramadol from the PAMAM G5 and PAMAM G5-FA dendrimers was examined at different pH (1.5, 7.4 and 8.5) at 37 °C. The percentage of drug release was obtained by extracting, at certain intervals of time, an aliquot of 2 mL from the buffer recipient containing the concentrations of morphine and tramadol liberated from the dendrimer-drug complexes. Each aliquot was analyzed by spectrophotometry to 285 nm and 270 nm, respectively. The analyses were done by triplicate and the percentage of error did not exceed 1%; thus, for clarity we do no show the error in the graphs.

The results for morphine delivery are shown in Fig. 3A–C. After eight hours, 51%, 29% and 21% of the morphine was released from amine-terminated PAMAM at pH 1.5, 7.4 and 8.5, respectively, whereas the release from PAMAM G5-FA at pH 1.5, 7.4 and 8.5 was 31%, 67% and 78%, respectively. 24 h after the experiment had, 97%, 45% and 30% of morphine was released from amine-terminate dendrimers at pH 1.5, 7.4 and 8.5, respectively. Meanwhile, at the same time, the percentage of drug released from PAMAM-G5-FA was 46% at pH 1.5, 94% at pH 7.4 and 92% at pH 8.5.

The information about the liberation of morphine from PAMAM G5-FA dendrimers is in agreement with studies done by Nakamura et al. [23] in which the *in vitro* liberation of morphine chlorohydrate of SPILA's granules (system of incorporation of caps of polymers) was evaluated pH 1.2 and 6.8. In this case, the liberation at acidic pH is slower than at neutral pH. The percentage of liberation at pH 6.8 was 80% at 6 h. Studies performed by Morales et al. [24] show that for Xantan, Carbapol and Carboximetilcelulosa of sodium, after 8 h, 50%, 67% and 81% of morphine were released, respectively, which is also in agreement with our study.

After 8 h, 61%, 20% and 19.5% of tramadol (Fig. 3D–F) was released from amine-terminated PAMAM at pH 1.5, 7.4 and 8.5 respectively, whereas that the release from PAMAM G5-FA at pH 1.5, 7.4 and 8.5 were 52%, 51% and 63%, respectively. 24 h after the experiment had begun, 91%, 55% and 49.5% of tramadol were been released from the amine-terminated dendrimers at 1.5, 7.4 and 8.5 pH values, respectively. At the same time, the release from PAMAM G5-FA was 69% at acid pH, 87% at neutral pH and 98% at basic pH.

It is necessary to notice, that as for morphine, the liberation of tramadol from the different dendrimers shows two phases: the

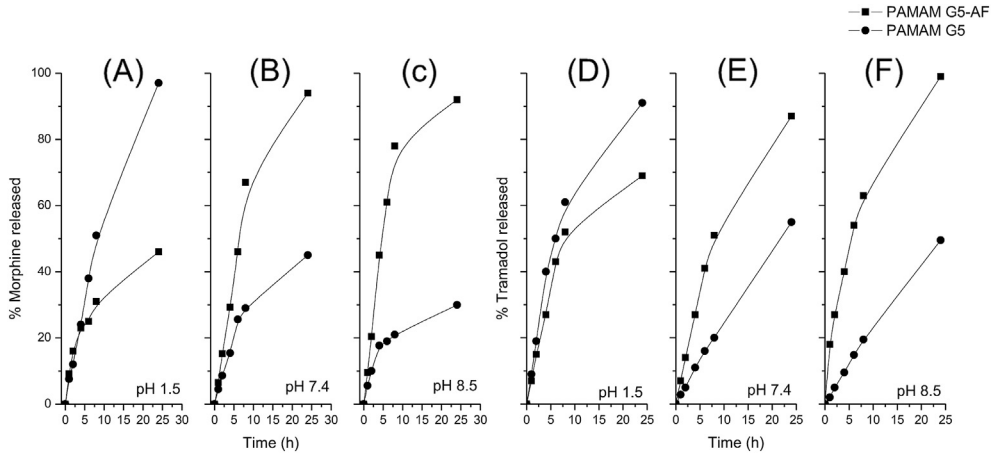

Fig. 3. (A) Morphine release at low (1.5), (B) neutral (7.4) and (C) high (8.5) pHs. (D) Tramadol release at low (1.5), (E) neutral (7.4) and (F) high (8.5) pHs.

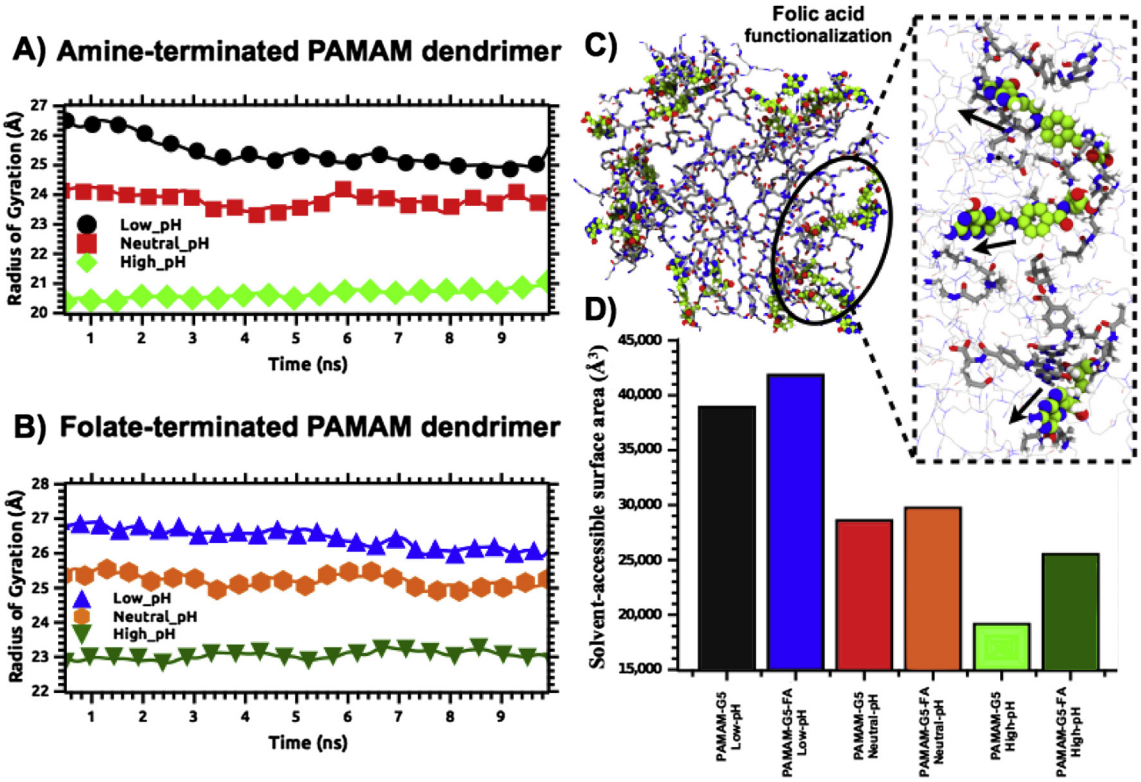

Fig. 4. Radius of gyration of (A) amine- and (B) folate-terminated PAMAM dendrimers at low, neutral and high pH as functions of time. (C) Representative snapshot of the orientation of the folic acid molecules on the outer surface of PAMAM dendrimers. The arrows indicate that folate groups are oriented towards the internal cavities of the dendrimer. Similar behavior was observed at the three distinct pH values. (D) Solvent-accessible surface area for each dendrimer at low, neutral and high pH.

rapid one, which can be associated with the release of the molecules located in the periphery of the dendrimers, and another slower phase, which likely is associated with release of the molecules located in a more internal region of the dendrimers. This phenomenon has been also suggested in previous studies considering other dendrimers and other drugs [25].

The release of morphine and tramadol from the PAMAM G5-FA/drug complex was appreciably slower at acid pH compared to the PAMAM G5/drug complex, allowing us to assume a better affinity of the drug with folate terminated dendrimers at this pH.

2.4. Drug release kinetics

To understand the mechanism by which the liberation of morphine and tramadol occurs from the different dendrimers, the average of the profiles of liberation obtained previously were adjusted through the Korsmeyer-Peppas [26] and Peppas-Sahlin [27] methods. The results obtained show that the coefficients of correlation (r) in all cases present a good adjustment to both mathematical models, although the Peppas-Sahlin model appears to be better (See Table SI1 and SI2 of Supporting information). The equation of Peppas-Sahlin, as it was mentioned previously, proposes two mechanisms of control of liberation. The first term of the equation corresponds to the contribution for the phenomenon of diffusion explained by Fick's law (K_d) and the second term corresponds to contribution for easing (K_r). The mechanism that prevails depends on the value of the constants. Moreover, due to the preponderance of K_d (contribution of Fickian mechanism) over K_r (contribution of the relaxation mechanism of the polymer chain), the drug-release mechanism from these dendrimers can be considered as the result of the joint contribution of a prevailing Fickian diffusion and the polymer chain relaxation. Diffusion in the classic Fickian limit is based on the supposition of a small mean-free-path (λ), rigorously speaking the limit Fickian it is equivalent $\lambda \rightarrow 0$ and this allows that the flows should be defined as gradients of density [24].

The prevalence of the contribution of the mechanism of Fickian diffusion (K_d) and the contribution of the mechanism of easing of the polymeric chains (K_r) were estimated, both for the amine- and folate-terminated PAMAM dendrimers, at the different pHs.

2.5. Molecular dynamics results

Structural analyses were performed on the last 10 ns of the trajectory of each simulated dendrimer, considering only the steady conformations. Fig. 4 shows the radius of gyration (R_g) and solvent-accessible surface area (SASA) as a function of the simulated time. The R_g characterizes the size of the dendrimers, giving a mean value of 25.9 ± 0.9, 24.2 ± 0.5 and 20.7 ± 0.2 Å for amine-terminated PAMAM at low, neutral and high pH, respectively (see Fig. 4A). These values are in accord with previous atomistic results [28–30] and show a direct relation to the charge of the dendrimers: the amines become deprotonated as pH increases, leading to a reduced charge and a more compact dendrimer. As shown in Fig. 4B, the behavior for folate-terminated (23 molecules) PAMAM dendrimers is similar, having mean R_g values of 26.5 ± 0.3, 25.2 ± 0.2 and 23.0 ± 0.1 Å at low, neutral and high pH, respectively. Despite the large size of folic acid molecules, the R_g of the dendrimers does not increase substantially upon addition of folate. A visual analysis of the trajectories of the MD simulation showed that the folate groups on the outer surface of the dendrimers are oriented inward and tend to penetrate into the cavities of the dendrimers. A snapshot illustrating this penetration is shown in Fig. 4C.

To evaluate the ability of dendrimers to encapsulate guest molecules, solvent-accessible surface area (SASA) analyses were performed. Fig. 4D shows that, at low pH, the SASA of the dendrimers is larger, implying that they adopt open conformations with large cavities to accommodate drugs. As pH increases, the dendrimers adopt a more compact structure; however, it appears that cavities for encapsulating drugs remain. These results are consistent with the radial mass densities, calculated for each dendrimer (see Fig. SI1). Compared with amine-terminated PAMAM, the folic-acid functionalized dendrimers show greater SASA values. At high pH, the SASA values of the folate-terminated dendrimers were nearly twice that of the amine-terminated dendrimers. The effect of folate-functionalization on the SASA was, however, less dramatic at low and neutral pH. It is often assumed that increases in SASA values are correlated with decreases in hydrophobicity [31]; thus, one could contend that the addition of the folate groups leads to PAMAM dendrimers of reduced hydrophobicity.

Considering the structural characteristics mentioned above, we randomly selected a cavity in each equilibrated dendrimer and expanded this cavity to a size sufficient to dock the drugs. Positive docking energies were calculated for both drugs at low pH, suggesting that stable complexes may not be formed between the dendrimers and either drug under these conditions. This instability is likely due to the fact that both the dendrimer and the drug are positively charged at low pH. However, at neutral and high pH, docking suggested stable complexes for all drug and dendrimer combinations. Therefore, although at low pH the dendrimers have sufficient cavities to encapsulate drugs, the polarity of morphine and tramadol prevents them from being encapsulated within the dendrimer.

Since docking results only allow us to observe trends in the affinity of dendrimer-drug complexes, the relative free binding energy was determined by the MM-GBSA method. Table SI3 shows details of the simulated systems and the free energy of binding for morphine and tramadol encapsulated in amine-terminated dendrimers at the three distinct pH values. The binding energies show that both morphine and tramadol have decreasing affinity with decreasing pH, which may be due to unfavorable electrostatic interactions at lower pH values. These results are in accordance with the release assays of the drugs, which show rapid release at low pH, a more gradual release at neutral pH, and the slowest release at high pH. We also observed that the energy values are lower for tramadol than for morphine, suggesting that tramadol forms a more stable complex with the dendrimers. However, the encapsulation assays showed a higher encapsulation proportion for morphine than for tramadol. We attribute the apparent disagreement to drug–drug interactions between tramadol molecules present in the experiments, resulting in lower encapsulation of this drug - it does not necessarily mean that the dendrimers have a greater affinity for morphine than tramadol.

In contrast to the experimental release assays for amine-terminated PAMAM, where the rate of release decreased with increasing pH, similar assays for folate-terminated PAMAM showed an increasing rate of release with increasing pH. On the contrary, the theoretical results in Table SI4 show that ΔG_{bind} of folate-terminated PAMAM has the same general tendency as that of amine-terminated PAMAM, that is, ΔG_{bind} decreases with pH. We explain this apparent discrepancy by a careful analysis of specific interactions in the dendrimer–drug complexes observed in the MD trajectories.

Visual inspection of the simulated complexes shows that drugs in the interior of the amine-terminated dendrimers at low pH are not in close contact with the dendrimer, presumably due to unfavorable electrostatic interactions, and remain almost fully solvated. Therefore, we observe lower intermolecular interactions, specifically hydrogen bonds, of the drugs with the amine-terminated dendrimer at low pH than at higher pH values. At neutral pH, despite the fact that drugs still have charge +1, the internal cavities of the dendrimers are neutral, allowing the formation of hydrogen bonds between the amide groups of the dendrimers and the hydroxyl/methoxy groups of the drugs (see Fig. SI2). However, we observed that when the drugs come in contact with the protonated amines an electrostatic repulsion promotes the elimination of the drug from the interior of the dendrimer. At high pH, both the amine-terminated dendrimer and the drugs are neutral, therefore, the dendrimer adopts a compact conformation, and the drugs form strong hydrogen bonds with the internal dendrons. Finally, both the experimental data and the binding energy values between the amine-terminated PAMAM dendrimers and the drugs directly correlate with the mean number of hydrogen bonds observed in the MD trajectories. In all cases, the order of affinity was: high pH > neutral pH > low pH.

For folate-terminated PAMAM dendrimer-drug complexes, the MD trajectories show that, at low pH, electrostatic repulsions are generated between the dendrons and the drugs, which is in accordance with the low affinity implied by the binding energies. However, we find no clear correlation between the binding energy predicted by MM-GBSA and the release rates measured in the experiments. The release of the drugs depends on both the binding energy and the local diffusion coefficient of the drugs within the dendrimer; thus, it is possible that the difference in the release rates between the folate-terminated and amine-terminated dendrimer are principally due to a difference in the rate of diffusion of the drugs within the two types of dendrimer. Unfortunately, the length of our simulations is not sufficient to discriminate differences in the diffusion coefficients that might be responsible for the different rates seen in Fig. 3. At acid pH, the folate-terminated complexes show higher affinity for the drugs than the amine-terminated complexes (Fig. 3A). The hydrogen bonds formed between the drugs and the internal cavities of the dendrimers, when morphine or tramadol reach the surface, ionic interactions are formed between the protonated amine of the drugs and the folates, which are negatively charged, the Fig. SI3 shows snapshots of intermolecular interactions, between the folate-terminated PAMAM and the drugs at neutral pH, most frequently observed along the MD simulations. At high pH, the amines of the dendrimers are neutral and the repulsion between the folate groups becomes important and causes a decreased in the hydrophobicity of the dendrimers. This phenomenon increase the entry of water molecules, which destabilize the hydrogen bonds, formed between the dendrimers and the drugs, promoting the release of the drugs from the inside.

3. Conclusions

PAMAM G5-FA was synthesized by surface modification of PAMAM G5. Mass spectrometry analysis confirmed that around 23 folic acid molecules were attached to PAMAM G5. The synthesized dendrimers were evaluated for controlled drug delivery of morphine and tramadol. It was found that PAMAM G5-FA improved characteristics for drug delivery property PAMAM G5. The amine and folate-terminated PAMAM-G5 dendrimers at different pH were studied by MD simulation techniques. The calculated R_g values were in agreement with previous atomistic results. Furthermore, functionalized PAMAM with folic acid showed sizes similar to non-functionalized PAMAM, due to the fact that the folate groups were oriented inward and tended to penetrate into the cavities of the dendrimer. For the other hand, folate groups on the surface decreased hydrophobicity of the dendrimers. The binding free-energy was calculated by MM-GBSA methods for each complex at

three different pH values. The binding energies between PAMAM G5 and morphine/tramadol were found to decrease with decreasing pH, a result in accord with the *in vitro* release assays of the drugs. For folate-terminated PAMAM complexes the binding free-energy did not clearly correlate with the experimental release data; however, the structural characterization showed that the intermolecular interactions are weakened as the pH increases which would explain the lower affinity of PAMAM G5-FA drugs *in vitro* at higher pHs. In brief, MD simulation techniques and the MM-GBSA method allow elucidation of the specific interactions that govern the stability and affinity of the dendrimer-drug complexes.

4. Material and methods

4.1. Materials

PAMAM G5 dendrimer was purchased in (Dendritech, Midland, MI), *N*-hydroxybenzotriazole (HOBt), 1-[3-(dimethylamine)propyl]-3-ethylcarbodiimide HCl (EDC), folic acid, dimethyl sulfoxide (DMSO) and *N*,*N*-dimethylformamide (DMF) were purchased from Sigma Aldrich Co. (Saint-Louis, MO, USA), dialysis membrane (M.W cut off of 500 Da) was purchased from Spectrum laboratories, Inc., Rancho Dominguez, CA.

4.2. Synthesis of folate–dendrimer conjugates

Conjugation of PAMAM G5 dendrimer with folic acid (FA) was carried out by a condensation between the γ-carboxyl group of FA and the primary amine group of PAMAM. Thus, 0.23 mmol of FA reacted with 1.28 mmol of EDC and HOBt in a mixture of dry DMF and dry DMSO under a nitrogen atmosphere for 1 h. The reaction mixture was added dropwise to a solution of 1.38×10^{-3} mmol of PAMAM in water. The reaction mixture was vigorously stirred for 72 h. The final functionalized dendrimer was purified through dialysis (using water) membranes with cut-offs of 500 Da to remove the excess folate.

4.3. Characterization of folate–dendrimer conjugates

Mass spectra of PAMAM G5 and PAMAM G5-FA dendrimers were carried out using Matrix-assisted laser desorption ionization–time of flight (MALDI–TOF). Mass spectra were recorded on a Bruker Ultraflex system equipped with a pulsed nitrogen laser (337 nm) (Bruker Daltonics Inc., Bremen Germany), operating in positive ion reflector mode, using a 19 kV acceleration voltage and a matrix of 2,5-dihydroxybenzoic acid. Cytochrome *c* (MW 12.361 Da), and apomyoglobin (MW 16.952 Da) were used as external standards. A dendrimer solution was prepared by dissolving 2 mg of dendrimer in 1 mL of DMSO. The matrix solution was prepared by dissolving 10 mg of matrix in 1 mL of the 1:1 mixture of deionized water and acetonitrile (0.1% TFA V/V). Analytical samples were prepared by mixing 10 μL of dendrimer solution with 100 μL of matrix solution, followed by deposition of 1 μL of sample mixture onto a MALDI plate. This mixture was allowed to air dry at room temperature (22–25 °C).

4.4. Drug loading into dendrimer conjugates

An excess of morphine and tramadol (1000 μM), in turn, was added to methanolic solution of PAMAM G5 and PAMAM G5-FA conjugates (1 μM) in screw-capped vials and the solution was kept at room temperature for overnight with constant agitation. For determining the amount of drug encapsulated in each dendrimer, the drug-loaded dendrimers were dissolved in CH_3OH and placed in a dialysis membrane bag (MW cut-off 500 Da). The bag was placed in 40 mL CH_3OH. Then the concentration of released Morphine or Tramadol untrapped was monitored using a UV spectrophotometer at 285 and 270 nm, respectively. The amount of morphine and tramadol encapsulated was determined indirectly [17].

4.5. In vitro release studies

In vitro drug release profiles of morphine and tramadol were determined as follows: the appropriate amount of drug-loaded dendrimer was suspended in three different buffer solutions (0.1 M HCl–KCl Buffer pH 1.5, 0.1 M PBS Buffer pH 7.4 and 0.1 M Tris–HCl Buffer pH 8.5)The drug-loaded conjugate solution (1 mL) was introduced into a dialysis membrane bag (MW cut-off 500 Da), then, the bag was placed in 40 mL of buffer solution release media, and the media was stirred at 37 °C. At predetermined intervals, 2 mL of sample was withdrawn and replaced with fresh 2 mL release medium. The drug concentration release (DR) into the different mediums as a function of time was monitored by UV-spectrophotometry at 285 nm and 270 nm for morphine and tramadol, respectively, and expressed as shown below:

$$\mathrm{DR}(\%) = M_t/M_\infty \times 100 \quad (1)$$

Where M_t is the drug amount released at time t and M_∞ is the total drug amount in the dendrimers. Experiments were performed in triplicate in order to minimize the experimental error.

4.6. Release models

In order to describe the rate of release of morphine and tramadol from the dendrimers, the data obtained from the *in vitro* release tests were fitted by two equations, including, Korsmeyer-Peppas's ($M_t/M_\infty = Kt^n$) [25] and Peppas-Sahlin's ($M_t/M_\infty = K_d t^n + K_r t^{2n}$) [26]. In all equations M_t and M_∞ are the absolute cumulative amounts of drug released at time t and at infinite time, respectively. In the Korsmeyer-Peppas's equation, K is a kinetic constant incorporating structural and geometric feature of the system, and the b term describes the burst effect (fast release from surface). In the Peppas-Sahlin's equation, K_d and K_r are constants, and the first term on the right hand side represents the Fickian diffusional contribution (F), whereas the second term represents the case-II relaxation contribution (R). In all these cases n is the diffusion exponent that can be related to the drug transport mechanism. For a spherical sample, when $n = 0.43$, the drug release mechanism is Fickian diffusion and when $n = 1.00$, the case II transport occurs, leading to zero-order release (polymer chains swelling or relaxing). When the value of n is between 0.43 and 1.00, anomalous transport is observed. These mathematical models were valid only for the first 60% of the drug release due to the burst effect related with the diffusion of the drug molecules in the surface samples [32].

4.7. Molecular dynamics simulations

4.7.1. Description of the dendrimer models

The initial structure for each dendrimer was built with ICM software [33] employing an *in silico* protocol similar to the divergent synthesis of dendrimers. Atomistic models of ethyldiamine-core and NH_2-terminated PAMAM dendrimers of fifth generation (G5) were built in three distinct protonation states: all amines protonated (low pH), only primary amines protonated (neutral pH) and fully deprotonated (high pH). Folate-terminated (~18%) PAMAM G5 dendrimers were generated under the same conditions.

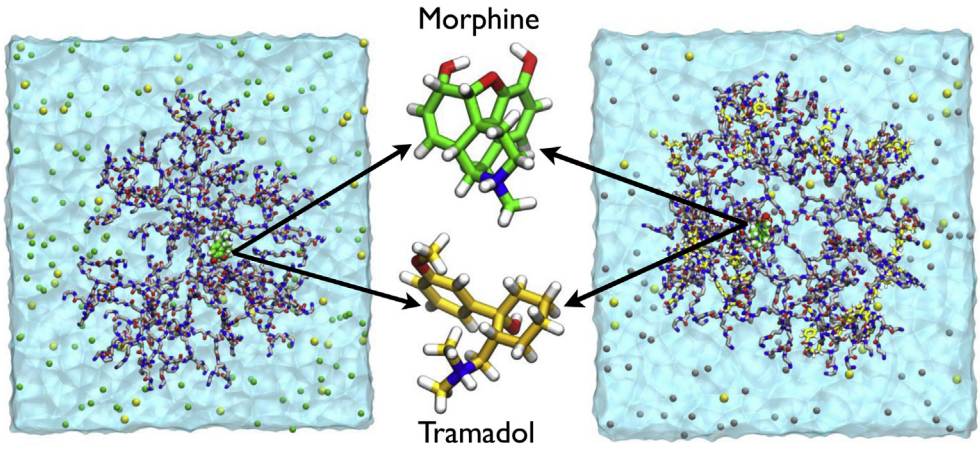

Fig. 5. Model of amine (left) and folate-terminated (right) PAMAM dendrimers in a box containing explicit water molecules (cyan) and 0.15 M NaCl. The dendrimer structures are shown by bond representation. The folic acid groups are shown in yellow (figure on the right). The NaCl ions are depicted as spheres, which are distributed in the solvent box. The drugs morphine and tramadol are shown in detail in the center of the figure. A similar setup was used in all simulations, including those at different pHs. (For interpretation of the references to color in this figure legend, the reader is referred to the web version of this article.)

The resulting structures underwent energy minimization and were relaxed through molecular dynamics (MD) simulations. For this purpose, it was necessary to parameterize each dendrimer based on the CHARMM27 [34] force field [35].

4.7.2. Drug insertion into the cavities

For the purpose of generate binding sites to encapsulate the drug within dendrimers, the equilibrated conformations of amine and folate-terminated PAMAM dendrimers were used to build empty cavities and simulate the encapsulation of morphine and tramadol drugs. Docking simulations using AutoDock 4.0 software [36] were carried out to insert the drug into each cavity and to find the preferred binding conformations of the drugs in the dendrimers. The parameters of Morphine and Tramadol (pK_a 8.00 and 9.41, respectively) were obtained from ParamChem [37]. In preparation for docking, a grid box was built large enough to accommodate free motion of the drug ($60 \times 60 \times 60$ Å^3). The grid parameters were generated using AutoGrid 4.0 and the Lamarckian Genetic Algorithm (LGA) was used to perform a search of the conformational space of the drugs. Ten conformations of each drug in complex with each dendrimer were obtained, which were finally analyzed with the program AutoDockTools [38] to select the best scoring docked conformation.

4.7.3. Molecular dynamic simulations of dendrimer-drug complexes

The lowest energy conformation of each complex obtained from Docking calculation was used as starting point to evaluate the specific interactions between dendrimers and drugs through MD simulation. Each dendrimer–drug complex was solvated in a periodic box ($\sim 100 \times 100 \times 100$ Å^3) of pre-equilibrated TIP3P [39] water molecules. Sodium and chloride ions were added to the aqueous phase to mimic physiological conditions (0.15 M NaCl) and to guarantee electric neutrality. The same protonation states and dendrimer parameters described above were used in all MD simulations. The initial configuration of each system (See Fig. 5) was optimized by energy minimization, followed by equilibration and relaxation through a ~15 ns MD simulation at 310 K in the isobaric-isothermal ensemble. Constant temperature was enforced using a Langevin thermostat with a damping coefficient of 1 ps^{-1}. Constant pressure (1 atm) was enforced using the Langevin piston method [40]. Short-range electrostatic and Van der Waals interactions were truncated smoothly at 12 Å, while long-range electrostatic forces were computed using the particle-mesh Ewald (PME) summation method [41]. The Verlet I r-RESPA multiple time-step integrator [42] was used with a time step of 2 fs. All molecular dynamics simulations were performed using the NAMD 2.9 software [43] with the standard ions and water of the CHARMM31 force field [33] and analyzed with VMD software [44]. The equilibration and data collection processes were monitored to obtain a sufficiently long trajectory to describe the structural and energetic properties.

4.7.4. MM-GBSA calculations of dendrimer–drug complexes

To estimate the relative binding free energy of the dendrimer-drug complexes the molecular mechanics (MM) generalized Born surface area (GBSA) method [45] was used. The MM-GBSA analysis was performed on three subsets of the system: the complex and the dendrimer and drug alone. For each one of these subsets, the free energy was calculated as follows:

$$G_{\text{tot}} = H_{\text{MM}} + G_{\text{solv-pol}} + G_{\text{solv-np}} - T\Delta S_{\text{conf}} \quad (2)$$

where H_{MM} and $G_{\text{solv-np}}$ correspond to the sum of mechanical energy terms and the polar contribution of solvation energy, respectively. Both terms were calculated by using NAMD 2.9 [40] with the generalized Born implicit solvent model [46] and the parameters described above. The dielectric constant of the solvent was set 78.5. The non-polar contribution of solvation energy was determined as a linear function of the solvent-accessible surface area (SASA), which was calculated with a probe radius of 1.4 Å [46]. The conformational entropy term should, in principle, be included; however it was not computed, due to the large computational cost. Finally, the binding free energy of each complex were calculated by the difference [47],

$$\Delta G_{\text{bind}} = G_{\text{tot}}(\text{complex}) - G_{\text{tot}}(\text{dendrimer}) - G_{\text{tot}}(\text{drug}) \quad (3)$$

Acknowledgments

We thank a partial contribution to the Programa Iniciativa Científica Milenio (ICM) del Ministerio de Economía, Fomento y Turismo, Fraunhofer Chile Research Foundation – Innova-Chile Corfo (FCR-CSB 09CEII-6991), and Proyecto Anillo Científico ACT1107. A.V.J. thanks the Doctoral Program of Applied Sciences of Talca University, as well as CONICYT-Chile for a doctoral fellowship. V.C.S. is in debt to CONICYT for doctoral fellowship No. 21121007

and University of Talca for Doctoral Program in Sciences. E.D.L. thanks to Fondecyt postdoctoral grant N°3120178.

Appendix A. Supplementary data

Supplementary data related to this article can be found at http://dx.doi.org/10.1016/j.ejmech.2013.11.040.

References

[1] D.A. Tomalia, Birth of a new macromolecular architecture: dendrimers as quantized building blocks for nanoscale synthetic polymer chemistry, Prog. Polym. Sci. 30 (2005) 294–324.
[2] S. Svenson, D.A. Tomalia, Dendrimers in biomedical applications-Reflections on the field, Adv. Drug. Deliv. Rev. 57 (2005) 2106–2129.
[3] Y.Y. Cheng, J.R. Wang, T.L. Rao, X.X. He, T.W. Xu, Pharmaceutical applications of dendrimers: promising nanocarriers for drug delivery, Front. Biosci. 13 (2008) 1447–1471.
[4] Y.Y. Cheng, Z.H. Xu, M.L. Ma, T.W. Xu, Dendrimers as drug carriers: applications in different routes of drug administration, J. Pharm. Sci. 97 (2008) 123–143.
[5] E.R. Gillies, J.M.J. Frechet, Dendrimers and dendritic polymers in drug delivery, Drug. Discov. Today 10 (2005) 35–43.
[6] J. Khandare, P. Kolhe, O. Pillai, S. Kannan, M. Lieh-Lai, R.M. Kannan, Synthesis, cellular transport, and activity of polyamidoamine dendrimermethylprednisolone conjugates, Bioconjug. Chem. 16 (2005) 330–337.
[7] P. Kolhe, J. Khandare, O. Pillai, S. Kannan, M. Lieh-Lal, R.M. Kannan, Preparation, cellular transport, and activity of polyamidoamine-based dendritic nanodevices with a high drug payload, Biomaterials 27 (2006) 660–669.
[8] H. Kobayashi, S. Kawamoto, P.L. Choyke, N. Sato, M.V. Knopp, R.A. Star, T.A. Waldman, Y. Tagaya, M.W. Brechbiel, Comparison of dendrimer-based macromolecular contrast agents for dynamic micro-magnetic resonance lymphangiography, Magn. Reson. Med. 50 (2003) 758–766.
[9] V.S. Talanov, C.A.S. Regino, H. Kobayashi, M. Bernardo, P.L. Choyke, M.W. Brechbiel, Dendrimer-based nanoprobe for dual modality magnetic resonance and fluorescence imaging, Nano. Lett. 6 (2006) 1459–1463.
[10] S. Svenson, Dendrimers as versatile platform in drug delivery applications, Eur. J. Pharm. Biopharm. 71 (2009) 445–462.
[11] C. Kojima, Design of stimuli-responsive dendrimers, Expert. Opin. Drug. Deliv. 7 (2010) 307–319.
[12] A. D'Emanuele, D. Attwood, Dendrimer–drug interaction, Adv. Drug. Deliv. Rev. 57 (2005) 2147–2162.
[13] A.E. Beezer, A.S.H. King, I.K. Martin, J.C. Mitchel, L.J. Twyman, C.F. Wain, Dendrimers as potential drug carriers; encapsulation of acidic hydrophobes within water soluble PAMAM derivatives, Tetrahedron 59 (2003) 3873–3880.
[14] A. Abderrezak, P. Bourassa, J.S. Mandeville, R. Sedaghat-Herati, H.A. Tajmir-Riahi, Dendrimers bind antioxidant polyphenols and cisplatin drug, PLoS One 7 (2012) 33102.
[15] Y. Wang, R. Guo, X. Cao, M. Shen, X. Shi, Encapsulation of 2-methoxyestradiol within multifunctional poly(amidoamine) dendrimers for targeted cancer therapy, Biomaterials 32 (2011) 3322–3329.
[16] Y. Zhang, T.P. Thomas, A. Desai, H. Zong, P.R. Leroueil, I.J. Majoros, J.R. Baker, Targeted dendrimeric anticancer prodrug: a methotrexate-folic acid-poly(-amidoamine) conjugate and a novel, rapid, "one pot" synthetic approach, Bioconjug. Chem. 21 (2010) 489–495.
[17] D. Chandrasekar, R. Sistla, F.J. Ahmad, R.P. Khar, P.V. Diwan, The development of folate-PAMAM dendrimer conjugates for targeted delivery of anti-arthritic drugs and their pharmacokinetics and biodistribution in arthritic rats, Biomaterials 28 (2007) 504–512.
[18] Y.Y. Cheng, T.W. Xu, R.Q. Fu, Polyamidoamine dendrimers used as solubility enhancers of ketoprofeno, Eur. J. Med. Chem. 40 (2005) 1390–1393.
[19] Y.Y. Cheng, Q.L. Wu, Y.W. Li, T.W. Xu, External electrostatic interaction versus internal encapsulation between cationic dendrimers and negatively charged drugs: which contributes more to solubility enhancement of the drugs, J. Phys. Chem. B 112 (2008) 8884–8890.
[20] O.M. Milhem, C. Myles, D. Attwood, A.J. D'Emanuele, Polyamidoamine Starburst dendrimers as solubility enhancers, Int. J. Pharm. 197 (2000) 239–241.
[21] S.C. Sweetman, P.S. Blake, Martindale: The Complete Drug Reference, 35th ed., Pharmaceutical Press, London, 2007.
[22] S. Grond, A. Sablotzki, Clinical pharmacology of tramadol, Clin. Pharm. 43 (2004) 879–923.
[23] K. Nakamura, E. Nara, T. Fuse, Y. Akiyama, Pharmacokinetic and pharmacodynamic evaluations of novel oral morphine sustained release granules, Biol. Pharm. Bull. 30 (2007) 1456–1460.
[24] M.E. Morales, G. Lopez, V. Gallardo, M.A. Ruiz, Oral suspensions of morphine hydrochloride for controlled release: rheological properties and drug release, Mol. Pharm. 8 (2011) 629–634.
[25] G.L. Aranovich, M.D. Donohue, Diffusion in fluids with large mean free paths: non-classical behavior between Knudse and Fickian limits, Phys. A: Stat. Mech. Appl. 388 (2009) 3355–3370.
[26] R.W. Korsmeyer, N.A. Peppas, in: J.T. Roseman, S.Z. Mansdorf (Eds.), Swelling-controlled Delivery Systems for Pharmaceutical Application: Macromolecular and Modeling Consideration, Controlled Release Delivery Systems, New York, 1983, pp. 77–79.
[27] N.A. Peppas, J.J. Sahlin, A simple equation for the description of solute release. III. Coupling of diffusion and relaxation, Int. J. Pharm. 57 (1989) 169–172.
[28] I. Lee, B.D. Athey, A.W. Wetzel, W. Meixner, J.R. Baker Jr., Structural molecular dynamics studies on polyamidoamine dendrimers for a therapeutic application: the effects of pH and generation, Macromolecules 35 (2002) 4510–4520.
[29] Y. Liu, V.S. Bryantsev, M.S. Diallo, W.A. Goddard, PAMAM dendrimers undergo pH responsive conformational changes without swelling, J. Am. Chem. Soc. 131 (2009) 2798–2799.
[30] K. Prabal Maiti, Tahir Çağın, S.T. Lin, A.G. William, Effect of solvent and pH on the structure of PAMAM Dendrimers, Macromolecules 38 (2005) 979–991.
[31] C. Chothia, The nature of the accessible and buried surfaces in proteins, J. Mol. Biol. 105 (1975) 1–12.
[32] P.L. Ritger, N.A. Peppas, A simple equation for description of solute release. II. Fickian and anomalous release from swellable device, J. Contr. Release 5 (1987) 37–42.
[33] R. Abagyan, M. Totrov, D. Kuznetsov, ICM-A new method for protein modeling and design: applications to docking and structure prediction from the distorted native conformation, J. Comput. Chem. 15 (1994) 488–506.
[34] A.D. Mackerell Jr., M. Feig, C.L. Brooks, Extending the treatment of backbone energetics in protein force fields: limitations of gas-phase quantum mechanics in reproducing protein conformational distributions in molecular dynamics simulations, J. Comput. Chem. 25 (2004) 1400–1415.
[35] J. Saam, I. Ivanov, M. Walther, H. Holzhütter, H. Kuhn, Molecular dioxygen enters the active site of 12/15-lipoxygenase via dynamic oxygen access channels, Proc. Natl. Acad. Sci. 104 (2007) 13319–13324.
[36] G.M. Morris, D.S. Goodsell, R.S. Halliday, R. Huey, W.E. Hart, R.K. Belew, A.J. Olson, Automated docking using a Lamarckian genetic algorithm and an empirical binding free energy function, J. Comput. Chem. 19 (1998) 1639–1662.
[37] K. Vanommeslaeghe, E. Hatcher, C. Acharya, S. Kundu, S. Zhong, J. Shim, E. Darian, O. Guvench, P. Lopes, I. Vorobyov, A.D. Mackerell Jr., CHARMM general force field: a force field for drug-like molecules compatible with the CHARMM all-atom additive biological force fields, J. Comput. Chem. 31 (2010) 671–690.
[38] G.M. Morris, R. Huey, W. Lindstrom, M.F. Sanner, R.K. Belew, D.S. Goodsell, A.J. Olson, AutoDock4 and AutoDockTools4: automated docking with selective receptor flexibility, J. Comput. Chem. 30 (2009) 2785–2791.
[39] W.L. Jorgensen, J. Chandrasekhar, J.D. Madura, R.W. Impey, M.L. Klein, Comparison of simple potential functions for simulating liquid water, J. Chem. Phys. 79 (1983) 926–935.
[40] S.E. Feller, Y.H. Zhang, R.W. Pastor, B.R. Brooks, Constant pressure molecular dynamics simulation – the Langevin piston method, J. Chem. Phys. 103 (1995) 4613–4621.
[41] U. Essmann, L. Perera, M.L. Berkowitz, T. Darden, H. Lee, L.G. Pedersen, A smooth particle mesh Ewald method, J. Chem. Phys. 103 (1995) 8577–8593.
[42] M.E. Tuckerman, B.J. Berne, G.J. Martyna, Reversible multiple time scale molecular dynamics, J. Phys. Chem. B 97 (1992) 1990–2001.
[43] J.C. Phillips, R. Braun, W. Wang, J. Gumbart, E. Tajkhorshid, E. Villa, C. Chipot, R.D. Skeel, L. Kalé, K. Schulten, Scalable molecular dynamics with NAMD, J. Comput. Chem. 26 (2005) 1781–1802.
[44] W. Humphrey, A. Dalke, K. Schulten, VMD: visual molecular dynamics, J. Mol. Graph 14 (1996) 33–38.
[45] N. Homeyer, H. Gohlke, Free energy calculations by the molecular mechanics Poisson–Boltzmann surface area method, Mol. Inf. 31 (2012) 114–122.
[46] D.E. Tanner, K.Y. Chan, J.C. Phillips, K. Schulten, Parallel generalized Born implicit solvent calculations with NAMD, J. Chem. Theory Comput. 7 (2011) 3635–3642.
[47] H. Abroshan, H. Akbarzadeh, G.A. Parsafar, Molecular dynamics simulation and MM–PBSA calculations of sickle cell hemoglobin in dimer form with Val, Trp, or Phe at the lateral contact, J. Phys. Org. Chem. 23 (2010) 866–877.